ELSEVIER
SAUNDERS

Neurol Clin 25 (2007) 439–471

NEUROLOGIC
CLINICS

Neck and Low Back Pain: Neuroimaging

Manzoor Ahmed, MD[a,*], Michael T. Modic, MD[b]

[a]*Department of Radiology, Louis Stokes VA Medical Center, 10701 East Boulevard, Cleveland, OH 44106-1702, USA*
[b]*Department of Radiology, Cleveland Clinic Foundation, 9500 Euclid Avenue, P34, Radiology, Cleveland, OH 44195, USA*

Neck and low back pain are among the most common medical disabilities in the Western world, with great economic and personal consequences [1]. According to a study by Hansson and Hansson [2], the annual total costs for back and neck problems can approximate 1% of the gross national product. Approximately 80% of the population suffers from back pain at some point in their lives [3], 80% get an imaging study, and 80% have nonspecific imaging findings. A significant portion of the cost of the morbidity associated with neck and back disorders is related to diagnostic testing. A significant component of this diagnostic testing is related to medical imaging, which is used to provide accurate morphologic information. Although degenerative changes of the spine are believed to be responsible for the majority of patient symptoms, they are not the only cause, and diagnostic imaging plays an important role in providing accurate diagnostic considerations. The ability to characterize these alterations better should provide a means of stratifying patient changes more accurately, thus a more accurate understanding of etiology. Not only are morphologic changes depicted in ever-increasing anatomic detail but also additional information is emerging that may help in understanding more fundamental alterations at the cellular and biochemical level. The impact of medical imaging on therapeutic decision making and cost effectiveness, however, other than as a presurgical tool, remains untested.

What separates individuals who have dramatic morphologic findings and who have no symptoms from individuals who have identical alterations and who do have symptoms? The relationship of etiologic factors, the morphologic alterations that can be characterized by imaging, and the mechanisms of pain production and their interactions in the production of symptoms all

* Corresponding author.
E-mail address: manzoor.ahmed@med.va.gov (M. Ahmed).

0733-8619/07/$ - see front matter
doi:10.1016/j.ncl.2007.01.007

are important and interactive factors. What follows is a review of the diagnostic imaging modalities used most commonly and their roles in patient management.

Imaging modalities

MRI

MRI currently is the test that provides the most information, albeit at a higher cost than other modalities. Using a variety of pulse sequences and paramagnetic contrast media, the extradural, intradural, and intramedullary spaces can be targeted. If the pathology is believed most likely in the extradural space, then a combination of T1, T2, and short tau inversion recovery (STIR)-weighted sequences is used. T2-weighted images provide myelographic-like display of epidural impressions by degenerative changes and sensitivity to intramedullary pathology. T1-weighted images allow a second type of contrast evaluation of the extradural structures, especially of the bone marrow and extradural soft tissue structures. STIR as a fat-suppression technique aids in the unmasking bone marrow, soft tissue edema, and infiltrative processes and provides another form of contrast for the detection of cord pathology. Gradient-echo images provide shorter scan times and sensitivity to susceptibility effects, as seen with blood by-products. Paramagnetic contrast agents are important for the detection of intramedullary disease, to assess the status of the spinal cord blood barrier. For extradural processes, such as spondylodiskitis and the postoperative spine, it can be useful in assessing epidural inflammation and fibrosis.

MR myelography generally uses a strong T2*-weighted sequence of 3-D–fast imaging with steady-state precession without intrathecal contrast injection. Although early studies have shown promise for the evaluation of nerve root compression and spinal stenosis by MR myelography [4–7], it is not used commonly in routine practice.

MR neurography uses high-resolution T1 imaging for anatomic detail, and fat-suppressed T2-weighted or STIR imaging to show abnormal nerve hyperintensity [8–10]. A wide variety of pathologies involving the sciatic nerve, such as compression, trauma, hypertrophy, neuromas, and tumor infiltration, may be seen [11,12]. MR neurography has demonstrated piriformis syndrome (piriformis muscle asymmetry and sciatic nerve hyperintensity) with a high specificity [13].

CT and other modalities

CT is an important modality in spinal imaging, with its greatest strength producing rapid, isotropic data sets, which can be post processed for evaluation of extradural disease. Without intrathecal contrast, it is insensitive to intradural and intramedullary disease. It is the most accurate modality for

the evaluation of bony detail. With multidetector systems, entire regions of the spine can be examined in seconds with slices as thin as 0.6 mm, providing highly accurate bony details in the evaluation of degenerative disease and fractures and for preoperative planning. CT is also highly accurate in anatomic assessment of spinal stenosis and disk herniation [14]. Plain radiography still holds a screening role in dynamic imaging (ie, flexion and extension views to evaluate alignment for instability). Although not yet popular, dynamic CT and MRI, using flexion, extension, axial loading, or standing in open MRI systems, have been performed with positive results [15–17].

Conventional myelography has been replaced almost completely by CT myelography, particularly with the advent of multidetector scanners [18]. The use of this procedure, which requires the instillation of a contrast medium intrathecally, currently is limited to preoperative confirmation of MR findings in selected cases, inconclusive MRI scans, postoperative instrumented spine disease, and patients who have MRI contraindications. The focus of the examination is assessment of epidural impressions on the thecal sac and filling of the nerve root sleeves. Dynamic CT myelography, using flexion extension positioning or axial loading to unmask positional stenosis, can be performed but is not yet accepted widely [16]. Provocative diskography is used for the evaluation of persistent back pain that is unexplained by other less invasive tests. It also is used for pre-fusion assessment to determine the status of disk spaces above and below levels of proposed fusion. The cardinal component of diskography is disk stimulation, not the morphology of the disk at diskography [19]. The criticism of diskography is related mainly to its invasive nature, reliability of the patient response, and lack of specificity [20–22].

Several radiologic procedures are promoted as techniques that provide localizing and therapeutic value in patients who have spine disease. Diagnostic nerve root and epidural injections are reported as having a high positive predictive value but low or indeterminate negative predictive value and specificity [23,24]. Diagnostic facet and sacroiliac joint blocks involve the instillation of local anesthetic around facet joint nerves (medial branch or dorsal ramus) and are reported to be reproducible, reasonably accurate, and safe. Some reports suggest that partial to complete pain relief for 6 months to 1 year may be achieved with facet block (see the article by Levin elsewhere in this issue) [25,26].

Neck pain, cervical radiculopathy, and myelopathy

The cervical spine is more flexible and mobile than the lumbar spine. The disk spaces are thinner, the canal and foramina are narrower, and there is less epidural fat in the cervical spine. Disk herniations are less common than in the lumbar region and associated more often with concomitant bony degenerative changes. Degenerative bony changes are seen in the vertebral bodies, facet joints, and the uncinate processes, which are designed to control translational motion of the cervical vertebrae.

Disk osteophyte complex

Osteophyte formation usually develops in the setting of disk herniation in cervical spine. The majority of osteophytic spurs contains bulging or frankly herniated disk material [27]. A disk-dominated complex has a better prognosis and greater tendency to regress spontaneously [28] than an extradural defect that is predominately bony (Fig. 1A, B).

Radiculopathy

Clinical assessment is critical for tailoring cervical examinations. Cervical radiculopathy should be distinguished clinically from other causes of neck and arm pain. Spondylotic radiculopathy is most common at C5-6 and C6-7. MR or CT with intrathecal contrast (CT myelography) is the most accurate imaging test. Plain film oblique views may identify foraminal encroachment from end-plate or uncovertebral joint and facet joint spurring but is insensitive to disk disease. CT is more sensitive to bony disease (Fig. 1C). Unexplained radiculopathy should prompt the search for foraminal or far lateral disk protrusions or osteophytes.

Myelopathy

Spondylotic compressive myelopathy is the most common cause of cord dysfunction in patients over 50 years of age. Other less common causes have toxic, metabolic, or neoplastic etiologies. The term, myelitis, which also results in cervical cord dysfunction, usually is reserved for infectious or

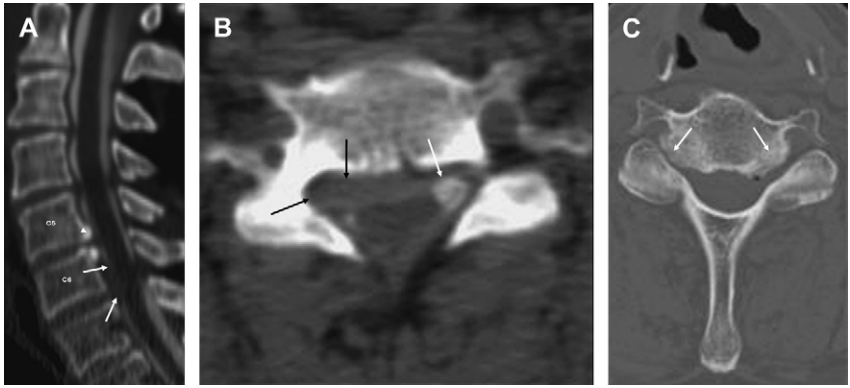

Fig. 1. Cervical degenerative disk disease. (*A*) Reconstructed sagittal CT myelogram—patient who had right C7 radiculopathy, anterior epidural defect dorsal to C6 body (*arrows*). (*B*) Axial CT myelogram, same patient—better shows thecal sac compression resulting from disk extrusion (*dark arrows*). Note intact left lateral recess thecal sac and nerve root (*white arrow*). Also, note bony dominant hypertrophic change at C5-6 (*A*) (*arrowhead*) with mild impression on thecal sac. (*C*) Axial nonmyelographic CT—different patient who had bilateral uncovertebral joint spurring (*arrows*) resulting in foraminal stenosis.

noninfectious inflammatory processes. MRI is the test of choice, as it can show not only cord compression but also intramedullary pathology. Sagittal T2 imaging supplemented by sagittal proton density, STIR, and axial T2 imaging is essential for diagnosis of intramedullary signal abnormality (Fig. 2).

Pyogenic cervical spondylodiskitis

Pyogenic cervical spondylodiskitis with or with out epidural abscess is more common than once believed [29]. Intravenous drug abuse is one of the most important risk factors [30]. Rarely, isolated epidural abscess is seen. There was a high incidence of multilevel involvement and epidural abscesses in a study of pyogenic cervical spine infections by Friedmand and colleagues [31]. MRI with and without contrast is the study of choice. Given the smaller cervical disk spaces and potential anatomic space in the prevertebral soft tissues, the dominant findings in cervical spondylodiskitis comprise prevertebral edema or abscess with minimal disk space or endplate marrow changes. Sagittal STIR images are the most sensitive sequence for the detection of subtle prevertebral edema and inflammation. True abscess formation usually is manifested by peripheral enhancement of a fluid collection versus confluent epidural soft tissue enhancement, which is more typical of a phlegmon (Fig. 3).

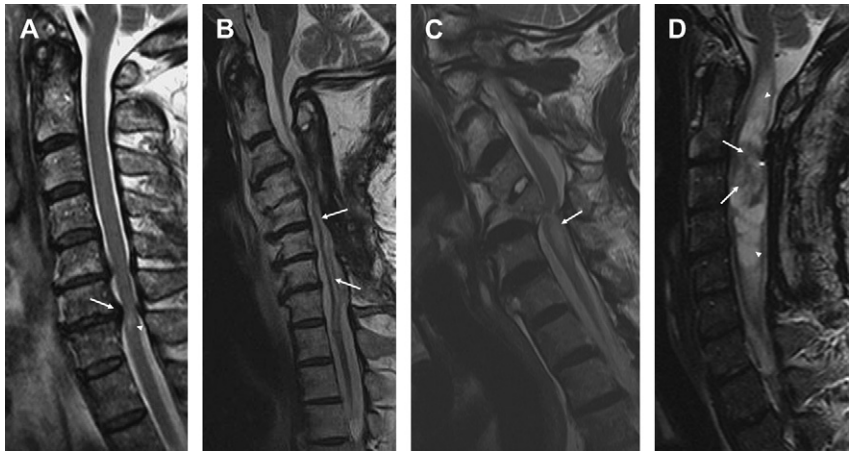

Fig. 2. Cervical melopathy: sagittal T2 images. (*A*) Posterior disk bulging or protrusion at C6-7 (*arrow*), mildly flattening the cord; associated focal signal abnormality (*arrowhead*) representing spondylotic myelomalacia. (*B*) Extensive myelomalacia (*arrows*) as a sequela of spondylosis and perioperative vascular compromise. Patient status post extensive posterior decompression at C3-7. (*C*) AS with collapsed C5 vertebra; note cord swelling and signal abnormality (*arrow*) resulting from compression by C5 retropulsion. (*D*) Ependymoma. Sagittal T2—expansile heterogenous mass (*arrows*) with marked cord edema (*arrowheads*).

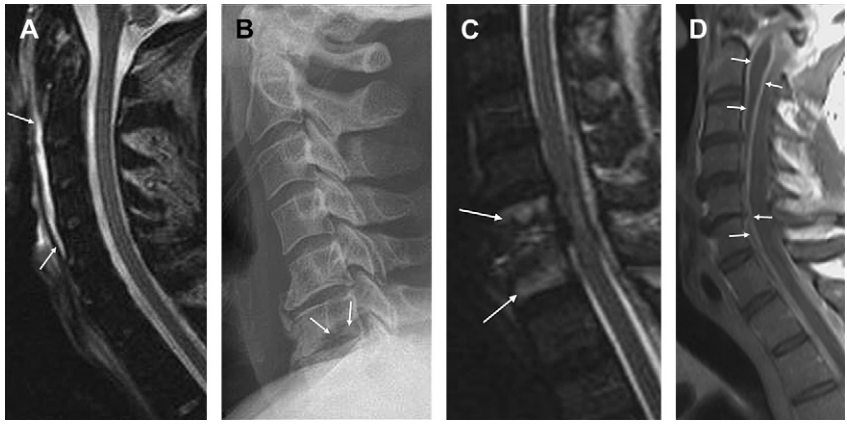

Fig. 3. Cervical spine infection. (*A*) Prevertebral abscess. Sagittal STIR with prevertebral T2 hyperintensity (*arrows*), later proved to be the result of C1-2 infection, not quite apparent on this examination. (*B, C*) DO. Lateral plain film (*C*)—focal end-plate erosion (*arrows*). Sagittal T2 (*C*)—C6-7 T2 hyperintensity in the vertebral bodies and disk space (*arrows*) resulting from DO. (*D*) Epidural abscess. Sagittal T1 post contrast—different patient who had spontaneous rim-enhancing extensive anterior epidural fluid collection (*arrows*).

Atlantodental and upper cervical spine disease

The atlantodental intervertebral level is unique as it lacks a typical disk space. It is the level most proximate to skull base. A soft tissue ligamentous complex supports the atlantodental joint. These structures give rise to the manifestations of a group of disorders. In rheumatoid arthritis, C1-2 is affected in approximately 20% to 25% of patients, resulting in neck or occipital pain, and may cause compressive myelopathy [32,33]. Typical imaging features of subluxation (usually anterior) and odontoid erosion are displayed on conventional radiographs and reformatted sagittal and coronal CT images [34]. On MRI, intermediate T1 and T2 signal intensity changes with diffuse enhancing pannus are seen, encroaching on the subarachnoid space and compressing the cord (Fig. 4A) [35,36]. Hypertrophy degeneration results from advanced osteoarthritis, calcium pyrophosphate deposition, or the sequela of chronic instability, with pseudopannus or pseudotumor formation mimicking rheumatoid arthritis [37]. Advanced age, hypertrophic bony changes, and nonenhancement of the retrodental soft tissue suggest degenerative etiology (Fig. 4B). Tuberculous spondylitis preferentially involves the craniovertebral junction and C1-2, with potential for bone destruction and large spinal or paraspinal soft tissue fluid collections and masses [38–40]. Atlantodental involvement in ankylosing spondylitis (AS) is common, with radiologic findings, including atlantodental calcification, subluxation, or ossification [41,42]. Upper cervical spine/C2 fracture in AS, although uncommon, may be seen (Fig. 4C). Spondyloarthropathy in long-term hemodialysis patients, also termed destructive spondyloarthropathy, commonly affects the

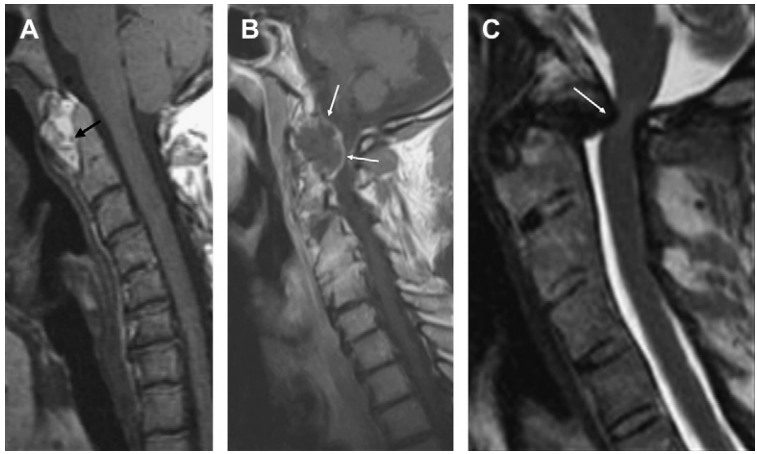

Fig. 4. Atlantodental and upper cervical spine disease. (*A*) Rheumatoid arthritis. Sagittal T1 post contrast–predental enhancing pannus (*arrow*). (*B*) Pseudopannus sagittal T1 post contrast—retrodental degenerative soft tissue hypertrophy with compression of the cord. Dorsal rim enhancement (*arrows*) likely related to epidural venous plexus. The soft issue was calcified on CT (not shown). Patient was asymptomatic. (*C*) AS. Sagittal T2 dental fracture and compromise of the foramen magnum (*arrow*).

midcervical spine with erosive end-plate changes and also causes atlantodental subluxation and pseudopannus. On MRI, there are intermediate T1 and T2 signal intensity changes secondary to amyloid deposition [43–45].

Prevertebral edema-related disorders

There are several disorders that cause acute neck pain and manifest as prevertebral soft tissue thickening and T2 hyperintensity or edema. Spondylodiskitis is discussed previously. Acute ligamentous injury resulting from flexion or extension injury may be seen without fractures. STIR-weighted sequences are the most sensitive for the detection of prevertebral or posterior paraspinal edema, indicative of ligamentous injury and neck sprain (Fig. 5A). Retropharyngeal cellulites, with or without true abscess, is a pediatric disorder related to tonsillopharyngeal pathology. It is rare in adults [46] but should be considered in immunocompromised patients who have neck pain, fever, and prevertebral edema. Calcific retropharyngeal tendonitis is a rare self-limited entity resulting from inflammation of longus colli muscles, with acute onset of severe pain localized in the back of the neck and aggravated by head movements and swallowing. Prevertebral edema with amorphous calcific deposits is characteristic (Fig. 5B, C) [47–49].

Back pain and lumbar radiculopathy

Back pain and lumbar radiculopathy are the main reasons for referral for spine imaging. Unfortunately, abnormalities on spine imaging are common

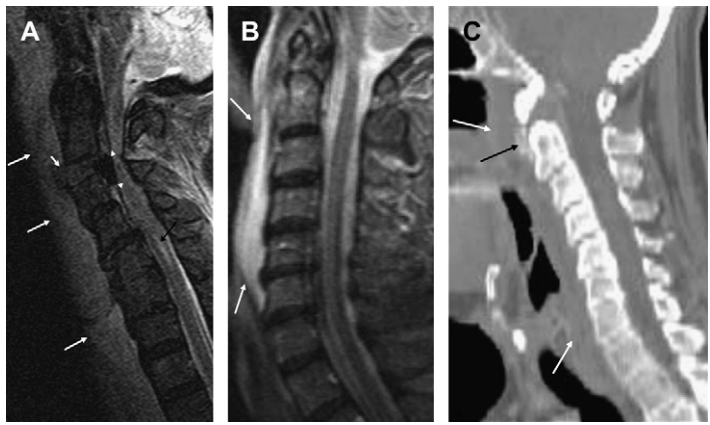

Fig. 5. Prevertebral edema. (*A*) Acute ligamentous injury. Sagittal T2—severe spinal trauma resulting from flexion extension injury with extensive prevertebral edema (*long white arrows*), anterior ligamentous disruption (*small white arrow*), posterior ligamentous disruption and epidural hematoma (*small white arrowheads*), and diffuse cord contusions (*dark arrow*). CT was negative for fractures. (*B*, *C*) Longus colli calcific tendonitis–extensive prevertebral edema on sagittal T2 (*A*) (*arrows*) and prevertebral focal calcification (*dark arrow*) on reconstructed sagittal CT soft tissue neck image (*B*). Note prevertebral edema on CT (*B*) (*white arrows*).

and nonspecific [50–52]. This cloud of nonspecificity superimposed on the multifactorial nature of the back pain poses a perpetual diagnostic and therapeutic challenge to clinicians and radiologists. The causes of symptoms related to the lower spine are diverse. Back pain and lumbar radiculopathy are the most common symptoms. The pain usually is attributed to (1) instability associated with disk degeneration, facet hypertrophic arthopathy; (2) mechanical compression of nerves by bone, ligament, or disk material; and (3) biochemical mediators of inflammation or pain. There is innervation of the outer layers of the intervertebral disk, which is responsible for the pain generation [53,54]. Superimposed reparative changes alter the anatomy, however, triggering pathologic nociceptive innervation and increased pain. Compression of the nerve roots, alternatively, lead to venous stasis, edema, and, ultimately, intraneural and perineural fibrosis [55]. This article's discussion on thoracolumbar spine imaging focuses on degenerative disease, followed by a brief review of other common disorders responsible for back pain.

Degenerative lumbar spine disease

Anatomic factors

Each spinal level is a three-joint complex with the anterior column (intervertebral joint between the end plates) and the two facet joints of the posterior column supported by ligaments and muscle groups. The zygoapophyseal (facet) joints and intervertebral disk joints act as an interactive functional unit, perpetually exposed to mechanical stresses, leading to

degeneration of the osseomyocartilagenous complex [56], resulting in characteristic imaging manifestations. The dynamism at these joints, termed microinstability, is hypothesized to result in progressive loss of strength in the joint capsules, leading to degeneration with reactive osteocartilaginous hypertrophy and disk changes [57]. The inter-relationship of these elements is important, as evident from the ongoing transition of surgical procedures from joint fusion to joint replacement [58].

Etiology of disk degeneration

The disk is metabolically active and the metabolism is dependent on diffusion of fluid from the marrow of the vertebral bodies across the subchondral bone and cartilaginous end plate or through the annulus fibrosus from the surrounding blood vessels. Disk degeneration is linked primarily to mechanical loading with mechanical factors producing end-plate changes, considered a precursor to disk changes [59,60]. Mechanical, traumatic, and nutritional factors all play roles in the cascade of disk degeneration to variable degrees in individuals. Genetic factors play a role in disk degeneration [61–64]. Whatever the cause, by 50 years of age, more than 80% of adults show evidence of degenerative disk disease at autopsy [65]. MRI can track the evolutionary changes in disk degeneration, but the distinction between aging changes and pathologic changes remains unclear [66].

Terminology

Reports point the tendency for interobserver and intraobserver variations in spine imaging interpretation [66–69]. This is related partly to inconsistency in the terminology. In this review, the terms used follow the recommendations of Milette [68]. Spondylosis deformans refers to the consequences of normal aging affecting mainly the annulus fibrosus and adjacent apophyses with anterior and lateral osteophytosis. Intervertebral osteochondrosis, or deteriorated disk, represents a pathologic process affecting primarily the nucleus pulposus and end plates, different from fissuring of the annulus fibrosus and reactive or erosive changes in the end plates [70,71].

A transitional vertebra occurs at the junction between two types of vertebral bodies, such as at the lumbosacral junction. A transitional vertebra demonstrates characteristics of both types of vertebrae, usually involving the vertebral arch or transverse process, and usually involves a partial fusion between the two vertebrae. It has an incidence in the general population ranging from 5% to 30% [72–74]. An association with back pain is reported [75]. A transitional lumbar (L5) or sacral (S1) vertebra may be fused partially or completely with the sacrum or lumbar spine, respectively. Recognition of a transitional vertebra is crucial to appropriate localization before invasive procedures.

Degenerative disk-space changes

An intervertebral disk is composed of an inner portion, the nucleus pulposus, and a peripheral portion, the annulus fibrosus. With degeneration

and aging, there is loss of the hydrostatic properties of the disk, resulting primarily from increasing type II collagen and alteration in the proteoglycans [76–78]. Although morphologic changes of the disk space readily are characterized on MRI studies, their relationship with patient symptoms cannot be interpreted. Loss of disk space T2 signal intensity is an early and common MRI sign of disk degeneration (Fig. 6A). In addition, the demarcation of hypointense outer layers of annulus fibrosus from the central zone of inner annular layers and the nucleus pulposus is blurred or lost [79]. Vacuum phenomenon and disk calcification, easily identified on plain radiographs or CT, contribute to disk space T2 signal loss. Disk space narrowing, identified readily on plain radiographs, develops as a result of progressive disk dessication.

Annular disk bulging, also described as broad-based disk protrusion, typically is visualized as a concentric bulge, sometimes with lateral or posterior asymmetry. Disk bulges and protrusions generally are incidental findings [51]. Impressions on the thecal sac or cord, however, do contribute to central canal stenosis, particularly in the presence of posterior element hypertrophy (PEH). Pseudo disk bulging is seen in the setting of anterolisthesis, as a result of uncovering of the disk at the posterior margin of the end plates.

Annular disk tear, commonly as a radial tear, is manifested by focal T2 hyperintensity in the setting of posterior disk bulging or protrusion. Such a disk signal abnormality is a strong predictor of annular tears [80,81]. Although some investigators correlate this abnormality with the presence

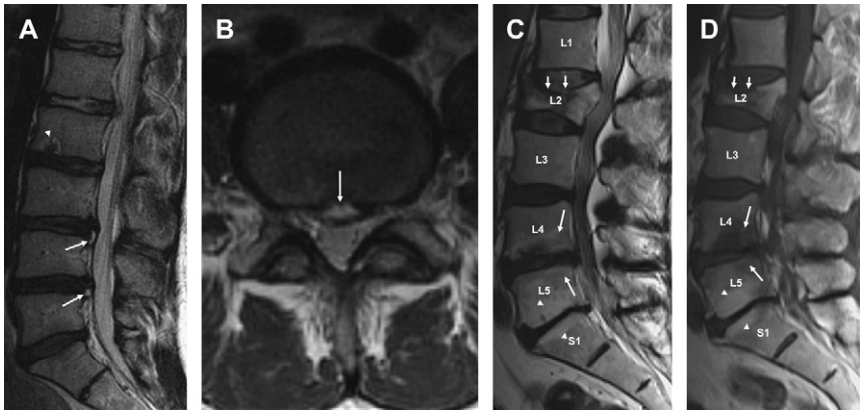

Fig. 6. Degenerative disk disease. (*A*) Sagittal T2—posterior annular disk bulges and protrusions with annular tears as T2 hyperintensities (*arrows*). Note near complete loss of T2 signal in L4-5 disk space. Arrowhead pointing to Schmorl's node. (*B*) Axial T2 broad-based disk protrusion with annular tear (*arrow*). (*C, D*) Degenerative end-plate bone-marrow changes. Sagittal T2 (*C*) and T1 (*D*) showing type I (*arrows*) and type II (*arrowhead*) changes. Note remote L2 benign compression deformity (*small arrows*).

of back pain [80,82], it has been shown to occur in up to 60% of asymptomatic patients (see Fig. 6A; Fig. 6B) [81,83].

Degenerative end-plate marrow changes

Type I changes represent granulation tissue and show decreased T1 and increased T2 end plates signal intensity. Type II changes, more common than type I changes, represent fatty marrow replacement and show increased signal on T1- and T2-weighted images. Type III changes correlate with extensive bony sclerosis on plain radiographs and show decreased signal intensity on T1- and T2-weighted images (see Fig. 6C–D) [84–86].

Degenerative facet and ligamentous changes

Disease of facet joints (including sacroiliac joints) is identified in 15% to 40% of patients who have chronic low back pain [23,87,88]. Like all diarthrodial synovium–lined joints, the lumbar facet joints are predisposed to arthropathy related to damage to articular cartilage. CT is the study of choice to detect and characterize facet arthropathy using thin axial slices generating high quality 3-D images. The typical features of arthritis include joint space narrowing, irregularity or osteophytosis, vacuum phenomenon, and sclerosis (Fig. 7A). Spondylolysis may be seen along with advanced hypertrophic arthropathy. MRI sagittal T2 images show rostrocaudal subluxation (contributing to foraminal stenosis), and axial T2 images demonstrate joint effusion and associated findings, such as synovial cysts and ligamentum flavum hypertrophy (LFH) or laxity. Synovial cysts projecting into the posterolateral spinal canal may impinge the cord, thecal sac, or nerve roots significantly. Synovial cysts demonstrate variable T1 and T2 signal depending on their proteinaceous fluid content, identified by their origin from facet joints and their rounded contours (Fig. 7B, C).

Important ligaments of the spine include the anterior longitudinal ligament, the posterior longitudinal ligament, the paired sets of ligamenta flava (connecting the laminae of adjacent vertebrae), intertransverse ligaments (extending between transverse processes), and the unpaired supraspinous ligament (along the tips of the spinous processes). LFH is a common contributor to morphologic central canal stenosis, especially when coexistent with facet.

Morphologic and functional sequelae of degenerative changes

Disk herniation

Disk herniation is a broad term encompassing different types and degrees of intervertebral disk displacement. Disk protrusion has many synonyms, such as disk prolapse or herniated nucleus pulposus. Protrusion is limited more strictly to a bulge less than or equal to 25% of disk circumference, but the

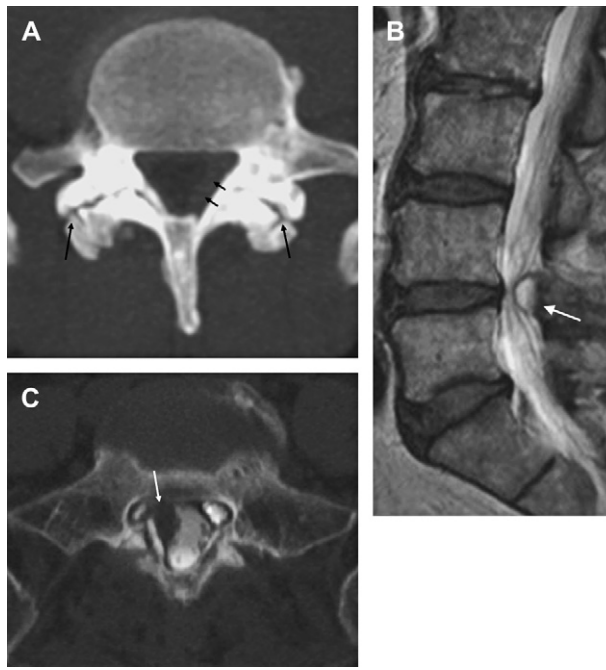

Fig. 7. Facet joints. (*A*) Facet arthropathy. Axial CT. Bilateral hypertrophic facet joint changes (*long arrows*) in an asymptomatic patient. Note faintly visualized ligamentum flavum thickening (*small arrows*). (*B, C*) Synovial cyst. Sagittal T2 (*B*)—a rounded cystic lesion (*arrow*), which on axial CT myelogram (*C*) shows right-side posterior epidural impression on thecal sac, abutting the facet joint (*arrow*).

term generally is used for any degree of focal lateral, foraminal, or posterior disk bulge with primary focus on abutment, compression, or displacement of the thecal sac and nerve roots (see Fig. 6B). Protrusion is the displacement of the nucleus pulposus and inner annular material through the annulus but not through the outer-most annular fibers. Its high prevalence in asymptomatic patients is evidence against its specific role in back pain [89].

A disk extrusion, considered a true herniated disk, extends through all the annular layers but remains connected with the primary disk material by a small isthmus or neck as the only attachment. A sequestered disk or free disk fragment is an extruded disk that has lost continuity with the primary disk. The fragment does not cross the midline because of a midline septum, but otherwise it can migrate anterior or posterior to the longitudinal ligament, lateral recess, neuroforamen, or thecal sac (intradural disk). Schmorl's nodes (herniations of the intervertebral disk through the vertebral end plates) usually are incidental findings but can been associated with back pain (see Fig. 6A) [90].

Foraminal and far lateral foraminal protrusions constitute 7% to 12% of all disk protrusions or extrusions and need more emphasis, as they can be overlooked clinically and on imaging. This subset of herniations, more

common at L3-4 and L4-5, can have more severe radicular signs on clinical examination [91,92]. Look for focal herniations in the foraminal and extraforaminal region on axial images and loss of foraminal fat on sagittal images (Figs. 8 and 9 show disk herniations).

Spinal instability

Segmental instability usually results from degenerative changes involving the intervertebral disk, vertebral bodies, or facet joints, causing impairment of the usual pattern of spinal movement and producing translational or angular motion that may be irregular, excessive, or restricted. Spondylolisthesis refers to displacement relative to the next most inferior vertebral body. Isthmic or spondylolytic spondylolisthesis is the most common type, with up to 50% to 60% of spondylolysis resulting in spondylolisthesis.

Spondylolysis refers to a defect in the pars interarticularis or isthmus and occurs with an incidence of approximately 3% to10% [93]. The majority of cases demonstrate bilateral L5 pars interarticularis defects, reflecting the uniform stress exerted by the body [94]. Lower lumbar spine spondylosis is unique to the human species because of upright posture, as spondylosis is not seen in individuals who have never walked [95,96]. Most isthmic defects appear in the first and second decades, reflecting the initial and more vigorous phases of activity in human life [93].

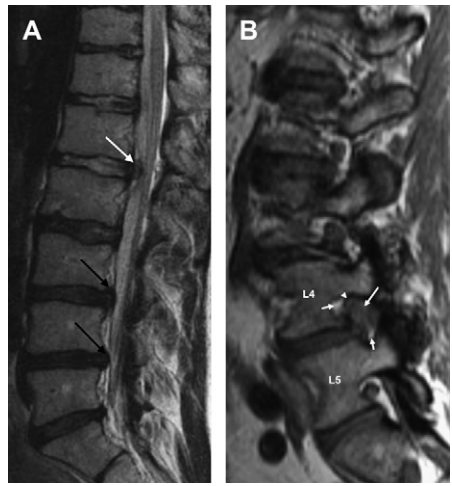

Fig. 8. Degenerative disk disease—sagittal imaging. (*A*) Postpartum 23-year-old patient who had cauda equina symptoms—sagittal T2 image showing L1-2 disc extrusion (*white arrow*) with moderate compression of thecal sac. Note diffuse disk degeneration with loss of normal T2 signal and annular disk bulges (*dark arrows*) in rest of the lumbar spine. (*B*) Sagittal T1—foraminal disk (*long arrow*) with foraminal stenosis; note L4 nerve root compression (*arrowhead*) and partial loss of hyperintense foraminal fat (*small arrows*).

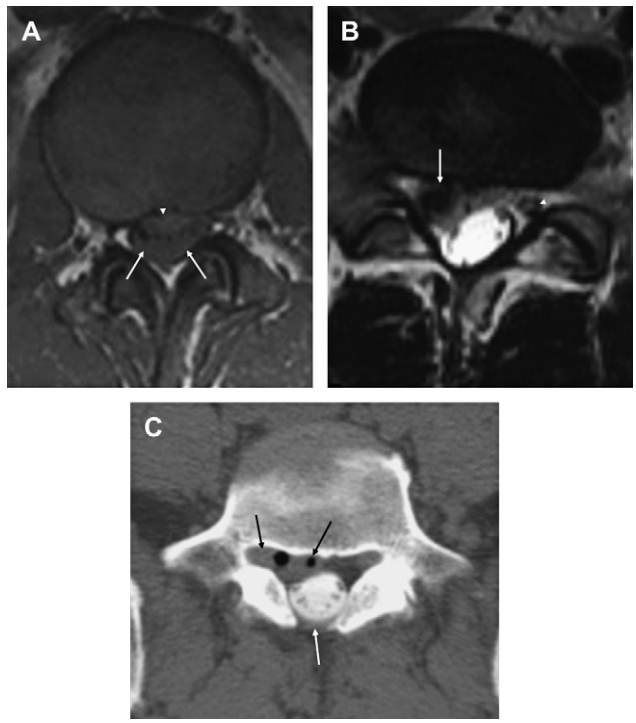

Fig. 9. Degenerative disk disease—axial imaging. (*A*) Axial T1—same patient as in Fig. 8A; disk extrusion compressing thecal sac (*arrow head*) with crowding of cauda equine nerve roots (*white arrows*). (*B*) Axial T2—a young resident physician who had acute right sciatica; note large disk extrusion (*white arrow*), compression of thecal sac and right S1 nerve root; left S1 nerve root is intact (*arrow head*). (*C*) Axial CT myelogram—different patient, mild thecal sac compression resulting from posterolateral disk protrusion with vacuum phenomenon (*dark arrows*); note decompression laminectomy (*white arrow*). Part of this epidural soft tissue impression is epidural scarring (see Fig. 19A).

Several studies address the question of the clinical significance of spondylolysis. Patients who have and who do not have back pain have a similar incidence of spondylolysis [97,98]. Approximately 25% of patients who have spondylolysis, however, eventually develop significant back pain during their lifetime [99]. Spondylolysis causes back pain in younger patients and predisposes to the development of disk and facet disorders in later life [100]. Oblique radiographs can detect defects in the pars interarticularis reliably, but thin-slice CT imaging with multiangled reformatting has improved accuracy, showing more defects compared with radiographs [101]. Single photon emission CT (SPECT) imaging is more effective in distinguishing between symptomatic and asymptomatic spondylolysis, and increased activity can aid in the localization of the source of pain [102,103]. MRI supplemented by fat saturation technique may show reversible signal

abnormalities in the pars interarticularis in the absence of defects, indicating a stress reaction associated with activity-related low back pain [104,105]. Detection of spondylolytic defects on MRI is difficult [106] unless there is associated retraction and anterolisthesis. Detection is aided by assessment of sagittal and axial images [107]. Spondylolysis may be observed on imaging without associated spondylolisthesis (Fig. 10).

Degenerative spondylolisthesis usually is identified in the presence of an intact pars interarticularis and is related primarily to degenerative changes of the apophyseal joints, most commonly at the L4-5 vertebral level. Degenerative disk disease may predispose to or exacerbate this condition because of narrowing of the disk space, which can lead to malalignment of the articular processes and rostrocaudal subluxation (Fig. 11).

Spinal canal stenosis

Spinal stenosis refers to narrowing of the spinal canal, lateral recesses or nerve root canals, or intervertebral foramina [108]. Two broad groups include acquired (usually caused by degenerative changes) and congenital or developmental. Some prefer the term, clinical stenosis, reflecting the importance of symptoms in establishing the diagnosis [109]. The imaging changes in general are more extensive than expected from the clinical findings [109]. There is no strong relationship between degree of stenosis and patient symptoms. Specific imaging findings do not predict benefit from surgery [110]. Position-dependent (dynamic) stenosis that worsens in extension and improves with flexion can be distinguished from static stenosis [109,111–113].

Congenital stenosis is explained primarily by shortened stubby pedicles with flattened axial appearance of the bony canal resulting from decreased anterior-posterior diameter along with narrowing of the lateral recesses and foramina [114]. Congenital stenosis usually is asymptomatic but reduces the reserve of the spine to accommodate degenerative hypertrophic changes during aging (Fig. 12). Acquired central canal stenosis in older patients typically is associated with disk and facet disease, disk bulges, and ligamentous hypertrophy and laxity. Degenerative spondylolisthesis and scoliosis also can contribute significantly to spinal stenosis. CT myelography with axial and multiplanar reformatted images provides greater detail than routine studies. Sagittal and axial MR images with T2 weighting allow accurate assessment of thecal sac compression (Fig. 13).

Acquired lateral recess stenosis is caused by disk–end-plate or superior articular facet hypertrophic changes. Asymptomatic nerve root contact may be seen with disk bulgings, protrusions, and osteophytosis. Contact by disk extrusion, however, is a significant finding [51,115]. Axial MRI or CT myelography shows a triangular-shaped normal lateral recess [116]. Facet and disk margin hypertrophic changes cause acute angled narrowing, whereas isolated facet hypertrophic arthropathy or PEH (which alone can cause radiculopathy) results in trefoil-shaped narrowing (Fig. 14) [117].

Fig. 10. Spondylolysis. (*A*) Isthmic spondylolysis.sagittal T1—grade I anterolisthesis of L5 on S1 (*arrow*) resulting from L5 pars interarticularis defect with retraction (*dark arrow*). (*B*) Bone scan. Axial SPECT—intense focal uptake right L5 pars interarticularis (*dark arrow*). (*C*, *D*) Pathologic spondylolysis. Sagittal T1—focal marrow replacement resulting from multiple myeloma (*C*) (*arrow*), transforming into pars defect on follow-up (*D*) (*arrow*); no retraction or anterolisthesis.

Acquired foraminal stenosis can be caused by lateral extension of disk bulging when associated with spondylosis, facet joint degenerative hypertrophic changes, or laxity (rostrocaudal subluxation). Loss of disk space height results in decreased vertical dimension of the foramina, whereas the sagittal dimensions are related to the sagittal dimensions of the pedicle and central canal [118]. Therefore, foraminal stenosis commonly is seen in association with canal stenosis. Sagittal MRI provides reliable assessment of the foramina [119] except in scoliosis. CT (preferably CT myelography) can complement the assessment and provide better demonstration of the bony foraminal canals.

Epidural lipomatosis is the accentuation of normal epidural fat, usually seen in the setting of endogenous or exogenous corticosteroid excess, and

Fig. 11. Degenerative spondylolisthesis: reconstructed panaromic sagittal CT myelogram—diffuse degenerative disk disease of the spine. Note mild retrolisthesis at L2-3 and anterolisthesis at L4-5 (*arrows*). Also note moderate degenerative central canal stenosis at L4-5.

is common in obese individuals. This usually is an incidental finding, but lipomatosis in the setting of structural stenosis can add to the compromise of the central canal. Rarely, epidural lipomatosis alone can lead to radiculopathy and cauda equina (Fig. 15) [120–122].

Cauda equina syndrome is related to simultaneous compression of multiple lumbosacral nerve roots below the level of the conus medullaris, resulting in a characteristic pattern of neuromuscular and urogenital symptoms. There are many potential causes, including epidural tumors, disk herniations, and epidural hematomas. Disk herniations account for approximately 1% of cases [123–125]. Acute onset of symptoms is a medical and surgical emergency [123,125]. MRI and myelography can demonstrate compression of the thecal sac reliably, whereas MRI also can characterize the cause of compression (Figs. 8A and 9A).

Significance of imaging findings in degenerative disease

The role of spine imaging is to provide accurate morphologic information and aid therapeutic decision making. Further advancements will aid in the understanding of underlying biochemical and cellular characteristics. Therapeutic decision making, however, is confounded by the high prevalence of morphologic changes in the asymptomatic population. Up to

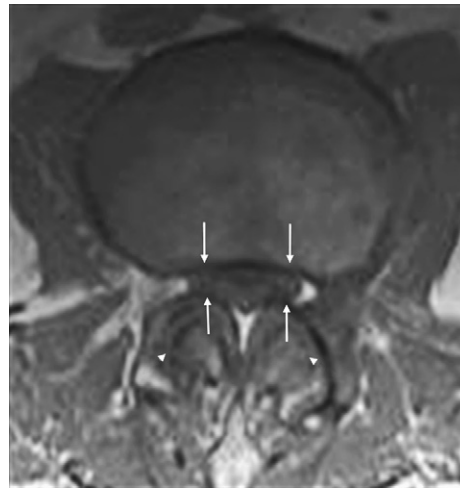

Fig. 12. Spinal stenosis: axial T1—congenital narrowing of the central canal; note decreased anteroposterior dimension of the canal (*arrows*) and stubby posterior elements (*arrowheads*).

30% of asymptomatic patients demonstrate disk herniations and most of them also have other degenerative change [51,126,127]. The MR findings do not by themselves correlate with the presence or duration of low back pain [128]. The incidence of disk herniations reaches up to 65% in patients

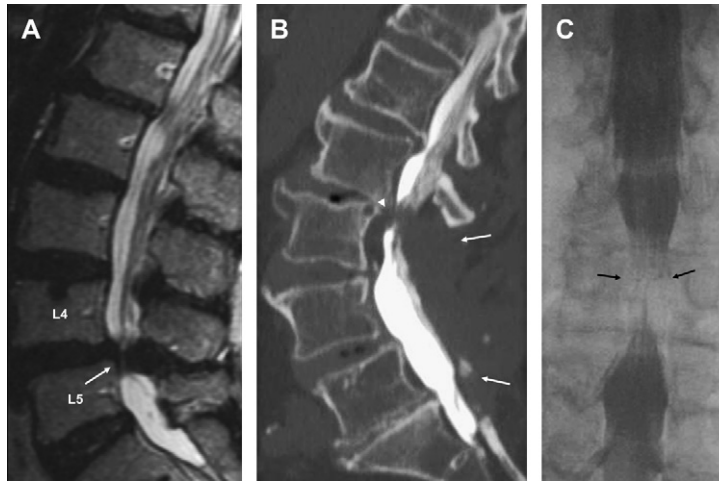

Fig. 13. Spinal stenosis. (*A*) Sagittal T2—severe central canal stenosis a result of mild disk bulging and dominant LFH at L4-L5. Note mild L4-5 anterolisthesis. (*B*, *C*) Acquired central canal stenosis. Sagittal CT myelogram (*B*)—severe thecal sac compression resulting from retrolisthesis and associated hypertrophic changes (*arrowhead*). Note lumbar spine decompression laminectomies (*arrows*). Corresponding conventional myelogram posterio-anterior image (*C*) showing thecal sac defect (*arrows*).

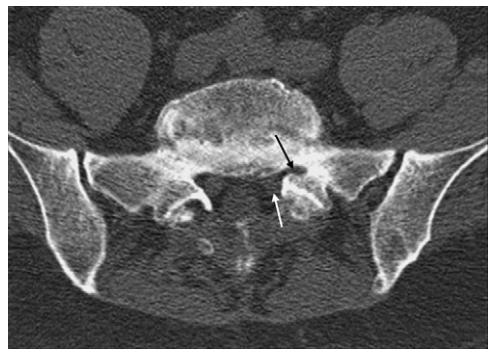

Fig. 14. Lateral recess stenosis: axial CT—left S1 lateral stenosis (*dark arrow*) resulting from facet joint hypertrophy; note the left S1 nerve is pushed medially (*white arrow*). The patient was asymptomatic.

who have back pain or radiculopathy [51,127]. Disk herniations can show dramatic reduction in size in patients undergoing conservative management [129,130]. There is no strong correlation between imaging and likelihood of clinical outcome [131]. In patients who have acute low back pain or radiculopathy, MRI does not seem to have measurable value in terms of planning conservative care [132]. The significance of bone marrow end-plate changes associated with degenerative disk disease is not clear. Type I changes, however, are shown to have a higher correlation with active low back symptoms

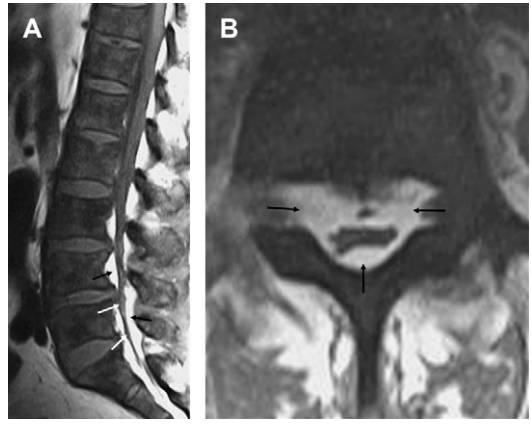

Fig. 15. Spinal epidural lipomatosis: sagittal (*A*) and axial (*B*) T1—epidural lipomatosis (*dark arrows*) with thecal sac compromise (*white arrows*) likely accounted for patient's symptoms as there was interval worsening of epidural lipomatosis after radiation therapy compared with previous examination (not shown); no epidural tumor was present. Note diffuse replacement of the normal fatty marrow resulting from prostatic metastatic disease.

[133–135]. Patients who have type I marrow changes and who undergo fusion for low back pain do better than those who do not have end-plate changes or type II patterns [133]. Furthermore, persistence of type I marrow changes after fusion is associated with significantly worse outcome [136]. Alternatively, conversion of type I marrow changes to a normal marrow signal or type II is correlated with good clinical results, successful fusion, and stabilization [133].

Diskitis osteomyelitis

Infection of the spine easily can be overlooked on clinical and imaging examinations during the early stages. Pyogenic and tuberculous spondylodiskitis have characteristic imaging features and can be differentiated to a considerable degree [137,138]. MRI is the study of choice.

Ledermann and colleagues [139] divide the imaging features of pyogenic diskitis osteomyelitis (DO) into two groups. First, disk-space changes including loss of disk space height and loss of central disk space nuclear cleft, but they are not very useful because of low sensitivity and specificity [139]. Hyperintense T2 signal in the disk space on MRI is, however, a sensitive marker of diskitis, but similar appearance in a hydrated degenerated disk is common in the authors' experience. Contrast enhancement in the disk space also is a highly sensitive marker and helpful in equivocal cases after noncontrast MRI; lack of disk space enhancement in DO is rare [137,140,141]. CT features usually are nonspecific unless there is advanced infection. DO should be suspected in cases of unusually prominent end-plate sclerosis. Look for end-plate lysis and collapse, better appreciated on sagittal reformations. The second group of imaging features is related to vertebral body and paraspinous soft tissues. MRI findings include hyperintense T2 and hypointense T1 end-plate bone marrow signal abnormality indicative of bone marrow edema and inflammation [139,142]. Partial to complete involvement of both vertebral bodies is common. Degenerative end-plate changes mimic spondylodiskitis by manifesting disk space hyperintensity and associated end-plate changes. Features favoring degenerative disease include more lateralized end-plate bone marrow signal abnormality with associated osteophytosis, lack of paraspinal soft tissue changes, or enhancement in the disk space. End-plate erosion is shown better on T1 images and may result in collapsed vertebra [142]. Paraspinal- and epidural-enhancing soft tissue thickening with or with out fluid collections is the most reliable imaging feature [142]. STIR (or other equivalent fat suppression techniques) can be helpful in unmasking the T2 hyperintensity in fat-rich paraspinal or epidural spaces and vertebral body marrow (Fig. 16). Tuberculous infection typically shows skip lesions, large paraspinal abscesses, vertebral collapse, and subligamentous spread [143,144].

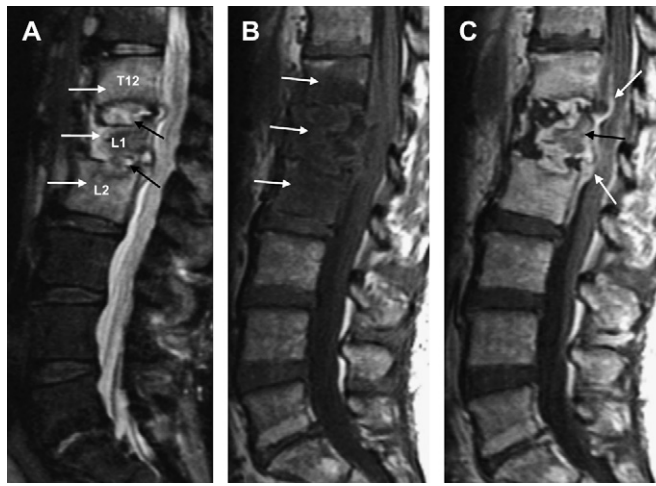

Fig. 16. DO. (*A*) Sagittal STIR—diffuse vertebral body marrow edema (*white arrows*) and disk spaces hyperintensity (*dark arrows*) at T12-L1 and L1-2; note mild compression deformity of L1. (*B*) Sagittal T1—corresponding diffuse T1 hypointensity in the vertebral bodies (*arrows*). (*C*) Sagittal post ontrast T1—diffuse rim enhancement of L1 representing osteomyelitis (*dark arrow*); note disk spaces enhancement and associated anterior epidural inflammatory enhancement/phlegmon (*white arrows*); no clear epidural abscess formation.

Compression fractures and bone marrow disease

The role of imaging in compression deformities is to determine recent versus chronic onset, compromise of the spinal canal resulting from retropulsion, and benign versus malignant etiology. Plain films have low sensitivity in detecting mild compression fracture deformities. Nuclear medicine bone scan findings are nonspecific and generally need correlation with morphologic studies. The usefulness of MRI in the evaluation of compression fractures lies in the detection of marrow edema, infiltrative changes, and associated paraspinal or epidural tumor. MRI can characterize and differentiate malignant from benign fractures in the majority of cases, facilitated by the findings of heterogeneous bone marrow signal and multilevel and multifocal marrow infiltration. Features highly in favor of malignant fractures include bulging contours, pedicle involvement, paraspinal soft tissue tumor, and marrow enhancement [145–147]. STIR sequences are helpful in identifying edema or tumor-related T2 hyperintensity (Fig. 17). Benign bone-marrow changes, such as patchy osteoporosis, reactive hematopoiesis, granulomatosis, or renal osteodystrophy, can mimic malignant infiltrative process (Fig. 18). Multidetector CT with 3-D imaging also can identify malignant fractures by identifying focal cortical or cancellous bone destruction and outlining the fracture deformities [148]. Percutaneous vertebroplasty and kyphoplasty are accepted methods of treatment of painful benign or

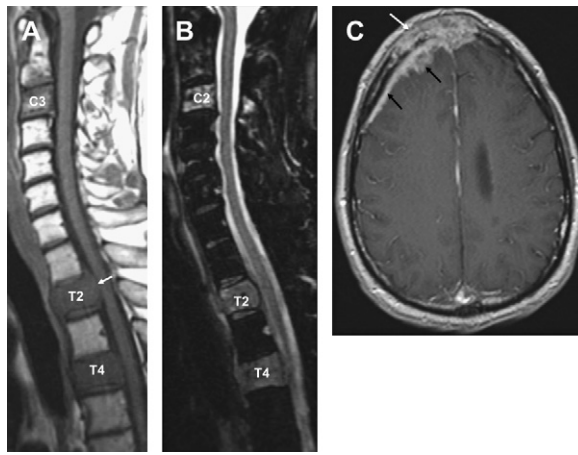

Fig. 17. Bone marrow disease: frontal sinus undifferentiated carcinoma with metastatic disease. (*A*) Sagittal T1—metastatic involvement of C3, T2, and T4. Note bulging contours at T2 and T4 and mild cord compression (*arrow*). (*B*) Sagittal STIR—corresponding hyperintense metastatic involvement. (*C*) Axial T1 postcontrast head—right frontal sinus and calvarial primary tumor (*white arrow*) with associated epidural intracranial extension (*dark arrows*).

pathologic compression fractures [149–152]; MRI and multiplanar CT are helpful in preoperative planning [153].

The postoperative spine

The United States has the highest incidence of spine surgery in the world, and it has increased over the past 2 decades [154]. There is an incidence of approximately 15% to 20% of failures, however, termed failed back syndrome [155–157]. Neuroimaging is important in this group of patients. MRI with and without contrast is the study of choice. CT myelography can be used in cases when MRI studies are inconclusive or degraded by artifact. Laminectomy is used most commonly for thecal sac decompression [158]; however, evidence of unilateral laminectomy, fenestration, or undercutting sometimes is difficult to identify on MRI. Look for attenuated ipsilateral ligamentum flavum or posterior bulge of the thecal sac into the defect. After fusion with or without instrumentation, several imaging findings can be seen. A posterolateral fusion has the appearance of clumps of corticated bone mimicking facet hypertrophic arthropathy. An interbody fusion has the appearance of partial to complete ankylosis of the disk space. Pseudoarthrosis (nonunion of the bony fusion) as assessed by MRI may be visualized poorly as a result of artifact from the cages. CT can be used to evaluate for bone formation or nonunion lucency around the cage [159]. Stabilizing fixation rods and screws are not a major limitation because of the current use of MRI-compatible metals, such as titanium. Disk

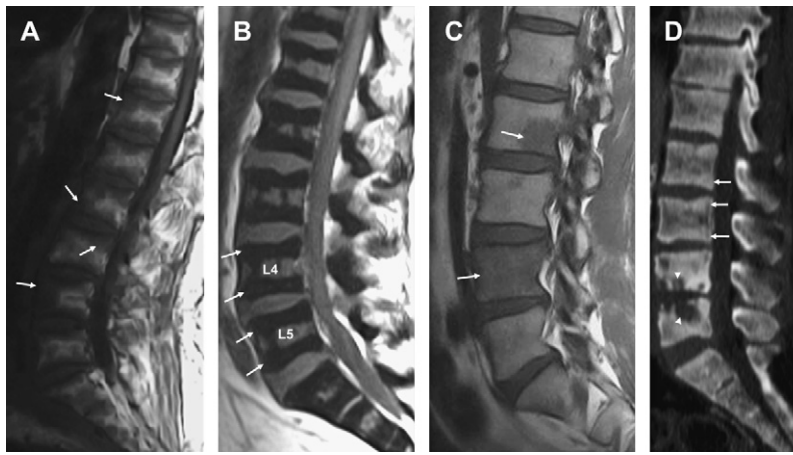

Fig. 18. Bone marrow disease. (*A*) Non-Hodgkin's lymphoma. Sagittal T1—diffuse patchy bone marrow replacement, mainly along the end plates (*arrows*). (*B*) Osteopetrosis. Sagittal T1—end-plates band-like hypointensity resulting from sclerosis (*arrows*), somewhat mimicking the appearance in (*A*). Note the uniform pattern indicating benign process. (*C*) Sarcoidosis. Sagittal T1—patchy to diffuse vertebral marrow replacement (*arrows*) with positive bone scan (not shown); biopsy showed granulomatous changes. (*D*) CT sagittal reformatted—band-like irregular sclerosis along the end plates (rugger jersey appearance) resulting from renal osteodystrophy (*arrows*). Note superimposed DO with bone erosion (*arrowheads*). Destructive spondyloarthropathy may have similar appearance.

replacement devices increasingly are used but with significant artifact degradation on MRI. Malpositioning and dislodgment of these devices can be observed on imaging (Fig. 19).

Recurrent disk herniation has an incidence of approximately 5% to 10%, generally defined as disk reherniation at the same level more than 6 months after surgery. Epidural scarring confounds imaging interpretation. In contrast to the localized bulging of a herniated disk, scarring shows a diffuse pattern with soft tissue replacement of normal epidural fat. A retractile configuration without mass effect favors epidural scarring [160]. Epidural scar typically manifests as diffuse enhancement, compared with marginal enhancement around a herniated disk, but differentiation can be difficult at times. CT myelography may be indicated as a complementary test (Fig. 20A).

A transitional phenomenon can occur as a result of a transitional level between the lower fused rigid spine and the upper flexible spine. This leads to progressive degeneration, advancing to anterior and posterior column segmental changes, termed pseudoarthrosis (distinct from nonunion of bony fusion, also referred to as pseudoarthrosis) (Fig. 20B).

Arachnoiditis is an adhesive fibrinous process involving the cauda equina. Multiple causes are described, including prior surgery, infection, intrathecal injections, and subarachnoid hemorrhage. Two patterns based on conventional myelography are described by Jorgensen and colleagues

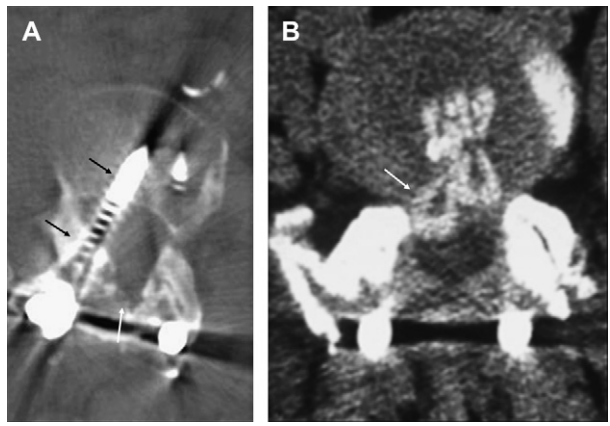

Fig. 19. Postoperative spine. (*A*) Malpositioned interpedicular screw. Axial CT—right side screw encroaching on the lateral recess of spinal canal (*dark arrows*). Note laminectomy defect (*white arrow*). (*B*) Displaced bone graft cage. Axial CT with intravenous contrast—focal compression of thecal sac by retropulsed cage (*arrow*).

[161]: type I, or featureless sac, with absence of nerve root defects, and type II, with localized or diffuse filling defects resulting from nerve roots clumping. On CT myelography or T2-weighted MRI, three patterns are described: central nerve root clumps or cords, lateral nerve root adhesions with empty

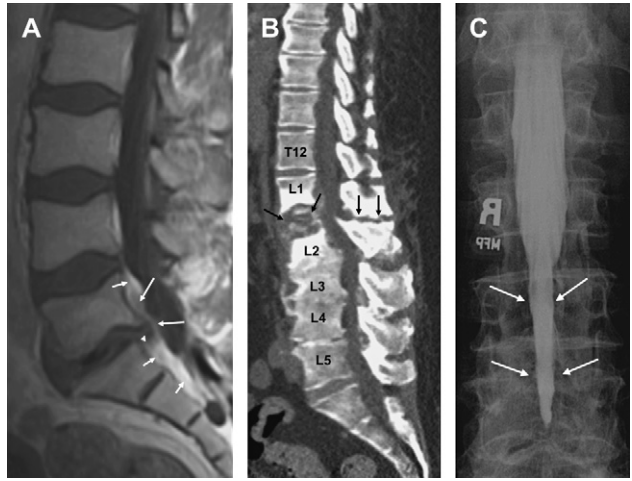

Fig. 20. Postoperative spine. (*A*) Epidural scar. Sagittal T1 post contrast—same patient as in Fig. 9C. Residual or recurrent small disk protrusion (*arrowhead*) surrounded by mildly enhancing epidural scarring (*long arrows*). Note more prominent surrounding hyperintensity resulting from epidural fat and enhancing epidural venous plexus (*small arrows*). (*B*) Pseudoarthrosis. Sagittal CT—L1-2 anterior and posterior column aligned lucency (*arrows*) resulting from abnormal motion. Note L2-3 and L3-4 anterior fusion. (*C*) Arachnoiditis. Conventional posterio-anterior myelogram—tapered lumbar myelographic block (*arrows*).

Fig. 21. Spinal dural AVF. (*A*) Sagittal T2 with distal cord edema (*long arrows*). Note surrounding prominent flow voids (*short arrows*). (*B*) Frontal view of left vertebral artery spinal angiogram. Note AVF (*white arrow*) and caudocranial flowing midline anterior spinal vein (*long dark arrows*) superimposed on anterior spinal artery fed by artery of cervical enlargement (*small dark arrows*).

thecal sac sign, and myelographic block with central mass-like appearance (Fig. 20C) [162].

Spinal arteriovenous malformations

Spinal arteriovenous malformations are rare. Clinical symptoms are believed related to venous hypertension, hemorrhage, steal phenomenon, or mass effect by varicosities. Back pain is an uncommon symptom, seen mainly in younger patients [163]. Classification focuses on the location of nidus or fistula (extradural, intradural, or intramedullary), the feeding arteries (single or multiple feeders), size of the nidus (compact or diffuse), and degree of shunting (low or high flow) [164–166]. A classification used commonly defines four types: type I (most common): dural arteriovenous fistula (AVF); type II: intramedullary glomus AVM; type III: juvenile or combined AVM; and type IV: intradural perimedullary AVF. Typical features on MRI include prominent intradural or extradural flow voids, cord edema, and perimedullary vascular and sometimes intramedullary enhancement related to venous hypertension and ischemia (Fig. 21A) [167,168]. Spinal angiography is used as confirmatory test and before endovascular treatment (Fig. 21B). Spinal MR angiography and CT angiography also are useful diagnostic tools [169–171].

References

[1] Kjellman G, Oberg B, Hensing G, et al. A 12-year follow-up of subjects initially sicklisted with neck/shoulder or low back diagnoses. Physiother Res Int 2001;6(1):52–63.

[2] Hansson EK, Hansson TH. The costs for persons sick-listed more than one month because of low back or neck problems. A two-year prospective study of Swedish patients. Eur Spine J 2005;14(4):337–45.
[3] Rish BL. A critique of the surgical management of lumbar disc disease in a private neurosurgical practice. Spine 1984;9(5):500–4.
[4] Hergan K, Amann T, Vonbank H, et al. MR-myelography: a comparison with conventional myelography. Eur J Radiol 1996;21(3):196–200.
[5] Eberhardt KE, Hollenbach HP, Huk WJ. 3D-MR myelography in diagnosis of lumbar spinal nerve root compression syndromes. Comparative study with conventional myelography. Aktuelle Radiol 1994;4(6):313–7 [in German].
[6] O'Connell MJ, Ryan M, Powell T, et al. The value of routine MR myelography at MRI of the lumbar spine. Acta Radiol 2003;44(6):665–72.
[7] Kuroki H, Tajima N, Hirakawa S, et al. Comparative study of MR myelography and conventional myelography in the diagnosis of lumbar spinal diseases. J Spinal Disord 1998; 11(6):487–92.
[8] Aagaard BD, Maravilla KR, Kliot M. Magnetic resonance neurography: magnetic resonance imaging of peripheral nerves. Neuroimaging Clin N Am 2001;11(1):viii, 131–viii, 146.
[9] Filler AG, Maravilla KR, Tsuruda JS. MR neurography and muscle MR imaging for image diagnosis of disorders affecting the peripheral nerves and musculature. Neurol Clin 2004; 22(3):643–vii.
[10] Maravilla KR, Bowen BC. Imaging of the peripheral nervous system: evaluation of peripheral neuropathy and plexopathy. AJNR Am J Neuroradiol 1998;19(6):1011–23.
[11] Moore KR, Tsuruda JS, Dailey AT. The value of MR neurography for evaluating extraspinal neuropathic leg pain: a pictorial essay. AJNR Am J Neuroradiol 2001;22(4):786–94.
[12] Ellegala DB, Monteith SJ, Haynor D, et al. Characterization of genetically defined types of Charcot-Marie-Tooth neuropathies by using magnetic resonance neurography. J Neurosurg 2005;102(2):242–5.
[13] Filler AG, Haynes J, Jordan SE, et al. Sciatica of nondisc origin and piriformis syndrome: diagnosis by magnetic resonance neurography and interventional magnetic resonance imaging with outcome study of resulting treatment. J Neurosurg Spine 2005;2(2):99–115.
[14] Bosacco SJ, Berman AT, Garbarino JL, et al. A comparison of CT scanning and myelography in the diagnosis of lumbar disc herniation. Clin Orthop Relat Res 1984;190:124–8.
[15] Jayakumar P, Nnadi C, Saifuddin A, et al. Dynamic degenerative lumbar spondylolisthesis: diagnosis with axial loaded magnetic resonance imaging. Spine 2006;31(10):E298–301.
[16] Yamazaki T, Suzuki K, Yanaka K, et al. Dynamic computed tomography myelography for the investigation of cervical degenerative disease. Neurol Med Chir (Tokyo) 2006;46(4):210–5.
[17] Weishaupt D, Boxheimer L. Magnetic resonance imaging of the weight-bearing spine. Semin Musculoskelet Radiol 2003;7(4):277–86.
[18] Tsuchiya K, Katase S, Aoki C, et al. Application of multi-detector row helical scanning to postmyelographic CT. Eur Radiol 2003;13(6):1438–43.
[19] Shah RV, Everett CR, McKenzie-Brown AM, et al. Discography as a diagnostic test for spinal pain: a systematic and narrative review. Pain Physician 2005;8(2):187–209.
[20] Carragee EJ, Alamin TF, Miller J, et al. Provocative discography in volunteer subjects with mild persistent low back pain. Spine J 2002;2(1):25–34.
[21] Carragee EJ, Lincoln T, Parmar VS, et al. A gold standard evaluation of the "discogenic pain" diagnosis as determined by provocative discography. Spine 2006;31(18):2115–23.
[22] Manchikanti L, Singh V, Pampati V, et al. Provocative discography in low back pain patients with or without somatization disorder: a randomized prospective evaluation. Pain Physician 2001;4(3):227–39.
[23] Hildebrandt J. Relevance of nerve blocks in treating and diagnosing low back pain—is the quality decisive? Schmerz 2001;15(6):474–83 [in German].
[24] North RB, Kidd DH, Zahurak M, et al. Specificity of diagnostic nerve blocks: a prospective, randomized study of sciatica due to lumbosacral spine disease. Pain 1996;65(1):77–85.

[25] Staender M, Maerz U, Tonn JC, et al. Computerized tomography-guided kryorhizotomy in 76 patients with lumbar facet joint syndrome. J Neurosurg Spine 2005;3(6):444–9.
[26] Manchkanti L, Pampati V, Fellows B, et al. Prevalence of lumbar facet joint pain in chronic low back pain. Pain Physician 1999;2(3):59–64.
[27] Miyasaka K, Isu T, Iwasaki Y, et al. High resolution computed tomography in the diagnosis of cervical disc disease. Neuroradiology 1983;24(5):253–7.
[28] Maigne JY, Deligne L. Computed tomographic follow-up study of 21 cases of non-operatively treated cervical intervertebral soft disc herniation. Spine 1994;19(2): 189–91.
[29] Shafaie FF, Wippold FJ, Gado M, et al. Comparison of computed tomography myelography and magnetic resonance imaging in the evaluation of cervical spondylotic myelopathy and radiculopathy. Spine 1999;24(17):1781–5.
[30] Endress C, Guyot DR, Fata J, et al. Cervical osteomyelitis due to i.v. heroin use: radiologic findings in 14 patients. AJR Am J Roentgenol 1990;155(2):333–5.
[31] Friedmand DP, Hills JR. Cervical epidural spinal infection: MR imaging characteristics. AJR Am J Roentgenol 1994;163(3):699–704.
[32] Semble EL, Elster AD, Loeser RF, et al. Magnetic resonance imaging of the craniovertebral junction in rheumatoid arthritis. J Rheumatol 1988;15(9):1367–75.
[33] Schwarz-Eywill M, Friedberg R, Stosslein F, et al. Rheumatoid arthritis at the cervical spine—an underestimated problem. Dtsch Med Wochenschr 2005;130(33):1866–70 [in German].
[34] Duan SY, Lin QC, Pang RL. Application of CT 3D reconstruction in diagnosing atlantoaxial subluxation. Chin J Traumatol 2004;7(2):118–21.
[35] Reijnierse M, Dijkmans BA, Hansen B, et al. Neurologic dysfunction in patients with rheumatoid arthritis of the cervical spine. Predictive value of clinical, radiographic and MR imaging parameters. Eur Radiol 2001;11(3):467–73.
[36] Stiskal MA, Neuhold A, Szolar DH, et al. Rheumatoid arthritis of the craniocervical region by MR imaging: detection and characterization. AJR Am J Roentgenol 1995;165(3): 585–92.
[37] Sze G, Brant-Zawadzki MN, Wilson CR, et al. Pseudotumor of the craniovertebral junction associated with chronic subluxation: MR imaging studies. Radiology 1986;161(2): 391–4.
[38] Krishnan A, Patkar D, Patankar T, et al. Craniovertebral junction tuberculosis: a review of 29 cases. J Comput Assist Tomogr 2001;25(2):171–6.
[39] Mariconda M, Lavano A, Ianno B, et al. Tuberculosis of the lower cervical spine: a description of two cases. Chir Organi Mov 1996;81(3):325–30.
[40] Wurtz R, Quader Z, Simon D, et al. Cervical tuberculous vertebral osteomyelitis: case report and discussion of the literature. Clin Infect Dis 1993;16(6):806–8.
[41] Lee JY, Kim JI, Park JY, et al. Cervical spine involvement in longstanding ankylosing spondylitis. Clin Exp Rheumatol 2005;23(3):331–8.
[42] Lee HS, Kim TH, Yun HR, et al. Radiologic changes of cervical spine in ankylosing spondylitis. Clin Rheumatol 2001;20(4):262–6.
[43] Chin M, Hase H, Miyamoto T, et al. Radiological grading of cervical destructive spondyloarthropathy in long-term hemodialysis patients. J Spinal Disord Tech 2006;19(6): 430–5.
[44] Kuntz D, Naveau B, Bardin T, et al. Destructive spondylarthropathy in hemodialyzed patients. A new syndrome. Arthritis Rheum 1984;27(4):369–75.
[45] Kiss E, Keusch G, Zanetti M, et al. Dialysis-related amyloidosis revisited. AJR Am J Roentgenol 2005;185(6):1460–7.
[46] Fogeltanz KA, Pursel KJ. Retropharyngeal abscess presenting as benign neck pain. J Manipulative Physiol Ther 2006;29(2):174–8.
[47] Karasick D, Karasick S. Calcific retropharyngeal tendinitis. Skeletal Radiol 1981;7(3): 203–5.

[48] Artenian DJ, Lipman JK, Scidmore GK, et al. Acute neck pain due to tendonitis of the longus colli: CT and MRI findings. Neuroradiology 1989;31(2):166–9.
[49] Mihmanli I, Karaarslan E, Kanberoglu K. Inflammation of vertebral bone associated with acute calcific tendinitis of the longus colli muscle. Neuroradiology 2001;43(12): 1098–101.
[50] van Tulder MW, Assendelft WJ, Koes BW, et al. Spinal radiographic findings and nonspecific low back pain. A systematic review of observational studies. Spine 1997;22(4):427–34.
[51] Jensen MC, Brant-Zawadzki MN, Obuchowski N, et al. Magnetic resonance imaging of the lumbar spine in people without back pain. N Engl J Med 1994;331(2):69–73.
[52] Videman T, Battie MC, Gibbons LE, et al. Associations between back pain history and lumbar MRI findings. Spine 2003;28(6):582–8.
[53] Edgar MA, Ghadially JA. Innervation of the lumbar spine. Clin Orthop Relat Res 1976; 115:35–41.
[54] Fagan A, Moore R, Vernon RB, et al. ISSLS prize winner: the innervation of the intervertebral disc: a quantitative analysis. Spine 2003;28(23):2570–6.
[55] Olmarker K, Rydevik B, Holm S. Edema formation in spinal nerve roots induced by experimental, graded compression. An experimental study on the pig cauda equina with special reference to differences in effects between rapid and slow onset of compression. Spine 1989; 14(6):569–73.
[56] Iida T, Abumi K, Kotani Y, et al. Effects of aging and spinal degeneration on mechanical properties of lumbar supraspinous and interspinous ligaments. Spine J 2002;2(2):95–100.
[57] Jane JA Sr, Jane JA Jr, Helm GA, et al. Acquired lumbar spinal stenosis. Clin Neurosurg 1996;43:275–99.
[58] Thalgott JS, Albert TJ, Vaccaro AR, et al. A new classification system for degenerative disc disease of the lumbar spine based on magnetic resonance imaging, provocative discography, plain radiographs and anatomic considerations. Spine J 2004;4(Suppl 6):167S–72S.
[59] Pritzker KP. Aging and degeneration in the lumbar intervertebral disc. Orthop Clin North Am 1977;8(1):66–77.
[60] Adams MA, Freeman BJ, Morrison HP, et al. Mechanical initiation of intervertebral disc degeneration. Spine 2000;25(13):1625–36.
[61] Hestbaek L, Iachine IA, Leboeuf-Yde C, et al. Heredity of low back pain in a young population: a classical twin study. Twin Res 2004;7(1):16–26.
[62] Annunen S, Paassilta P, Lohiniva J, et al. An allele of COL9A2 associated with intervertebral disc disease. Science 1999;285(5426):409–12.
[63] Marini JC. Genetic risk factors for lumbar disk disease. JAMA 2001;285(14):1886–8.
[64] Matsui H, Terahata N, Tsuji H, et al. Familial predisposition and clustering for juvenile lumbar disc herniation. Spine 1992;17(11):1323–8.
[65] Quinet RJ, Hadler NM. Diagnosis and treatment of backache. Semin Arthritis Rheum 1979;8(4):261–87.
[66] Brant-Zawadzki MN, Jensen MC, Obuchowski N, et al. Interobserver and intraobserver variability in interpretation of lumbar disc abnormalities. A comparison of two nomenclatures. Spine 1995;20(11):1257–63.
[67] Breton G. Is that a bulging disk, a small herniation or a moderate protrusion? Can Assoc Radiol J 1991;42(5):318.
[68] Milette PC. Reporting lumbar disk abnormalities: at last, consensus!. AJNR Am J Neuroradiol 2001;22(3):428–9.
[69] Raininko R, Manninen H, Battie MC, et al. Observer variability in the assessment of disc degeneration on magnetic resonance images of the lumbar and thoracic spine. Spine 1995; 20(9):1029–35.
[70] Twomey LT, Taylor JR. Age changes in lumbar vertebrae and intervertebral discs. Clin Orthop Relat Res 1987;224:97–104.
[71] Kirkaldy-Willis WH, Wedge JH, Yong-Hing K, et al. Pathology and pathogenesis of lumbar spondylosis and stenosis. Spine 1978;3(4):319–28.

[72] Elster AD. Bertolotti's syndrome revisited. Transitional vertebrae of the lumbar spine. Spine 1989;14(12):1373–7.
[73] Barzo P, Voros E, Bodosi M. Clinical significance of lumbosacral transitional vertebrae (Bertolotti syndrome). Orv Hetil 1993;134(46):2537–40 [in Hungarian].
[74] Luoma K, Vehmas T, Raininko R, et al. Lumbosacral transitional vertebra: relation to disc degeneration and low back pain. Spine 2004;29(2):200–5.
[75] Quinlan JF, Duke D, Eustace S. Bertolotti's syndrome: a cause of back pain in young people. J Bone Joint Surg Br 2006;88(9):1183–6.
[76] Adams P, Eyre DR, Muir H. Biochemical aspects of development and ageing of human lumbar intervertebral discs. Rheumatol Rehabil 1977;16(1):22–9.
[77] Brown MD. The pathophysiology of disc disease. Orthop Clin North Am 1971;2(2):359–70.
[78] Lipson SJ, Muir H. 1980 Volvo award in basic science. Proteoglycans in experimental intervertebral disc degeneration. Spine 1981;6(3):194–210.
[79] Modic MT, Pavlicek W, Weinstein MA, et al. Magnetic resonance imaging of intervertebral disk disease. Clinical and pulse sequence considerations. Radiology 1984;152(1):103–11.
[80] Peng B, Hou S, Wu W, et al. The pathogenesis and clinical significance of a high-intensity zone (HIZ) of lumbar intervertebral disc on MR imaging in the patient with discogenic low back pain. Eur Spine J 2006;15(5):583–7.
[81] Ricketson R, Simmons JW, Hauser BO. The prolapsed intervertebral disc. The high-intensity zone with discography correlation. Spine 1996;21(23):2758–62.
[82] Lam KS, Carlin D, Mulholland RC. Lumbar disc high-intensity zone: the value and significance of provocative discography in the determination of the discogenic pain source. Eur Spine J 2000;9(1):36–41.
[83] Derby R, Kim BJ, Lee SH, et al. Comparison of discographic findings in asymptomatic subject discs and the negative discs of chronic LBP patients: can discography distinguish asymptomatic discs among morphologically abnormal discs? Spine J 2005; 5(4):389–94.
[84] Modic MT, Steinberg PM, Ross JS, et al. Degenerative disk disease: assessment of changes in vertebral body marrow with MR imaging. Radiology 1988;166(1 Pt 1):193–9.
[85] de Roos A, Kressel H, Spritzer C, et al. MR imaging of marrow changes adjacent to end plates in degenerative lumbar disk disease. AJR Am J Roentgenol 1987;149(3):531–4.
[86] Chung CB, Vande Berg BC, Tavernier T, et al. End plate marrow changes in the asymptomatic lumbosacral spine: frequency, distribution and correlation with age and degenerative changes. Skeletal Radiol 2004;33(7):399–404.
[87] Manchikanti L. Facet joint pain and the role of neural blockade in its management. Curr Rev Pain 1999;3(5):348–58.
[88] Hodge JC, Bessette B. The incidence of sacroiliac joint disease in patients with low-back pain. Can Assoc Radiol J 1999;50(5):321–3.
[89] Boos N, Semmer N, Elfering A, et al. Natural history of individuals with asymptomatic disc abnormalities in magnetic resonance imaging: predictors of low back pain-related medical consultation and work incapacity. Spine 2000;25(12):1484–92.
[90] Masala S, Pipitone V, Tomassini M, et al. Percutaneous vertebroplasty in painful Schmorl nodes. Cardiovasc Intervent Radiol 2006;29(1):97–101.
[91] Lejeune JP, Hladky JP, Cotten A, et al. Foraminal lumbar disc herniation. Experience with 83 patients. Spine 1994;19(17):1905–8.
[92] Epstein NE. Foraminal and far lateral lumbar disc herniations: surgical alternatives and outcome measures. Spinal Cord 2002;40(10):491–500.
[93] Fredrickson BE, Baker D, McHolick WJ, et al. The natural history of spondylolysis and spondylolisthesis. J Bone Joint Surg Am 1984;66(5):699–707.
[94] Rothman SL, Glenn WV Jr. CT multiplanar reconstruction in 253 cases of lumbar spondylolysis. AJNR Am J Neuroradiol 1984;5(1):81–90.
[95] Kohlbach W. Spondylolysis/spondylolisthesis—a new thesis of its etiology. Rontgenblatter 1988;41(1):23–6 [in German].

[96] Rosenberg NJ, Bargar WL, Friedman B. The incidence of spondylolysis and spondylolisthesis in nonambulatory patients. Spine 1981;6(1):35–8.
[97] Porter RW, Hibbert CS. Symptoms associated with lysis of the pars interarticularis. Spine 1984;9(7):755–8.
[98] Pierce ME. Spondylolysis: what does this mean? A review. Australas Radiol 1987;31(4): 391–4.
[99] Wiltse LL. The effect of the common anomalies of the lumbar spine upon disc degeneration and low back pain. Orthop Clin North Am 1971;2(2):569–82.
[100] Cavalier R, Herman MJ, Cheung EV, et al. Spondylolysis and spondylolisthesis in children and adolescents: I. Diagnosis, natural history, and nonsurgical management. J Am Acad Orthop Surg 2006;14(7):417–24.
[101] Teplick JG, Laffey PA, Berman A, et al. Diagnosis and evaluation of spondylolisthesis and/or spondylolysis on axial CT. AJNR Am J Neuroradiol 1986;7(3):479–91.
[102] Collier BD, Johnson RP, Carrera GF, et al. Painful spondylolysis or spondylolisthesis studied by radiography and single-photon emission computed tomography. Radiology 1985; 154(1):207–11.
[103] Papanicolaou N, Wilkinson RH, Emans JB, et al. Bone scintigraphy and radiography in young athletes with low back pain. AJR Am J Roentgenol 1985;145(5):1039–44.
[104] Hollenberg GM, Beattie PF, Meyers SP, et al. Stress reactions of the lumbar pars interarticularis: the development of a new MRI classification system. Spine 2002;27(2): 181–6.
[105] Cohen E, Stuecker RD. Magnetic resonance imaging in diagnosis and follow-up of impending spondylolysis in children and adolescents: early treatment may prevent pars defects. J Pediatr Orthop B 2005;14(2):63–7.
[106] Saifuddin A, Burnett SJ. The value of lumbar spine MRI in the assessment of the pars interarticularis. Clin Radiol 1997;52(9):666–71.
[107] Campbell RS, Grainger AJ. Optimization of MRI pulse sequences to visualize the normal pars interarticularis. Clin Radiol 1999;54(1):63–8.
[108] Arnoldi CC, Brodsky AE, Cauchoix J, et al. Lumbar spinal stenosis and nerve root entrapment syndromes. Definition and classification. Clin Orthop Relat Res 1976;115:4–5.
[109] Amundsen T, Weber H, Lilleas F, et al. Lumbar spinal stenosis. Clinical and radiologic features. Spine 1995;20(10):1178–86.
[110] Treatment of degenerative lumbar spinal stenosis. Evid Rep Technol Assess (Summ) 2001; 32:1–5.
[111] Fujiwara A, An HS, Lim TH, et al. Morphologic changes in the lumbar intervertebral foramen due to flexion-extension, lateral bending, and axial rotation: an in vitro anatomic and biomechanical study. Spine 2001;26(8):876–82.
[112] Willen J, Danielson B, Gaulitz A, et al. Dynamic effects on the lumbar spinal canal: axially loaded CT-myelography and MRI in patients with sciatica and/or neurogenic claudication. Spine 1997;22(24):2968–76.
[113] Zander DR, Lander PH. Positionally dependent spinal stenosis: correlation of upright flexion-extension myelography and computed tomographic myelography. Can Assoc Radiol J 1998;49(4):256–61.
[114] Singh K, Samartzis D, Vaccaro AR, et al. Congenital lumbar spinal stenosis: a prospective, control-matched, cohort radiographic analysis. Spine J 2005;5(6):615–22.
[115] Jarvik JG, Hollingworth W, Heagerty PJ, et al. Three-year incidence of low back pain in an initially asymptomatic cohort: clinical and imaging risk factors. Spine 2005;30(13): 1541–8.
[116] Mikhael MA, Ciric I, Tarkington JA, et al. Neuroradiological evaluation of lateral recess syndrome. Radiology 1981;140(1):97–107.
[117] Bartynski WS, Lin L. Lumbar root compression in the lateral recess: MR imaging, conventional myelography, and CT myelography comparison with surgical confirmation. AJNR Am J Neuroradiol 2003;24(3):348–60.

[118] Cinotti G, De Santis P, Nofroni I, et al. Stenosis of lumbar intervertebral foramen: anatomic study on predisposing factors. Spine 2002;27(3):223–9.
[119] Cramer GD, Cantu JA, Dorsett RD, et al. Dimensions of the lumbar intervertebral foramina as determined from the sagittal plane magnetic resonance imaging scans of 95 normal subjects. J Manipulative Physiol Ther 2003;26(3):160–70.
[120] Robertson SC, Traynelis VC, Follett KA, et al. Idiopathic spinal epidural lipomatosis. Neurosurgery 1997;41(1):68–74.
[121] Qasho R, Ramundo OE, Maraglino C, et al. Epidural lipomatosis with lumbar radiculopathy in one obese patient. Case report and review of the literature. Neurosurg Rev 1997; 20(3):206–9.
[122] Ohta Y, Hayashi T, Sasaki C, et al. Cauda equina syndrome caused by idiopathic sacral epidural lipomatosis. Intern Med 2002;41(7):593–4.
[123] Ahn UM, Ahn NU, Buchowski JM, et al. Cauda equina syndrome secondary to lumbar disc herniation: a meta-analysis of surgical outcomes. Spine 2000;25(12):1515–22.
[124] Henriques T, Olerud C, Petren-Mallmin M, et al. Cauda equina syndrome as a postoperative complication in five patients operated for lumbar disc herniation. Spine 2001;26(3):293–7.
[125] Shapiro S. Medical realities of cauda equina syndrome secondary to lumbar disc herniation. Spine 2000;25(3):348–51.
[126] Wiesel SW, Tsourmas N, Feffer HL, et al. A study of computer-assisted tomography. I. The incidence of positive CAT scans in an asymptomatic group of patients. Spine 1984;9(6): 549–51.
[127] Boden SD, Davis DO, Dina TS, et al. Abnormal magnetic-resonance scans of the lumbar spine in asymptomatic subjects. A prospective investigation. J Bone Joint Surg Am 1990; 72(3):403–8.
[128] Borenstein DG, O'Mara JW Jr, Boden SD, et al. The value of magnetic resonance imaging of the lumbar spine to predict low-back pain in asymptomatic subjects: a seven-year follow-up study. J Bone Joint Surg Am 2001;83(9):1306–11.
[129] Saal JA, Saal JS, Herzog RJ. The natural history of lumbar intervertebral disc extrusions treated nonoperatively. Spine 1990;15(7):683–6.
[130] Modic MT, Ross JS, Obuchowski NA, et al. Contrast-enhanced MR imaging in acute lumbar radiculopathy: a pilot study of the natural history. Radiology 1995;195(2):429–35.
[131] Benoist M. The natural history of lumbar degenerative spinal stenosis. Joint Bone Spine 2002;69(5):450–7.
[132] Modic MT, Obuchowski NA, Ross JS, et al. Acute low back pain and radiculopathy: MR imaging findings and their prognostic role and effect on outcome. Radiology 2005;237(2): 597–604.
[133] Vital JM, Gille O, Pointillart V, et al. Course of Modic 1 six months after lumbar posterior osteosynthesis. Spine 2003;28(7):715–20.
[134] Weishaupt D, Zanetti M, Hodler J, et al. Painful lumbar disk derangement: relevance of endplate abnormalities at MR imaging. Radiology 2001;218(2):420–7.
[135] Braithwaite I, White J, Saifuddin A, et al. Vertebral end-plate (Modic) changes on lumbar spine MRI: correlation with pain reproduction at lumbar discography. Eur Spine J 1998; 7(5):363–8.
[136] Buttermann GR, Heithoff KB, Ogilvie JW, et al. Vertebral body MRI related to lumbar fusion results. Eur Spine J 1997;6(2):115–20.
[137] Maiuri F, Iaconetta G, Gallicchio B, et al. Spondylodiscitis. Clinical and magnetic resonance diagnosis. Spine 1997;22(15):1741–6.
[138] Jung NY, Jee WH, Ha KY, et al. Discrimination of tuberculous spondylitis from pyogenic spondylitis on MRI. AJR Am J Roentgenol 2004;182(6):1405–10.
[139] Ledermann HP, Schweitzer ME, Morrison WB, et al. MR imaging findings in spinal infections: rules or myths? Radiology 2003;228(2):506–14.
[140] Post MJ, Sze G, Quencer RM, et al. Gadolinium-enhanced MR in spinal infection. J Comput Assist Tomogr 1990;14(5):721–9.

[141] Dagirmanjian A, Schils J, McHenry M, et al. MR imaging of vertebral osteomyelitis revisited. AJR Am J Roentgenol 1996;167(6):1539–43.
[142] Modic MT, Feiglin DH, Piraino DW, et al. Vertebral osteomyelitis: assessment using MR. Radiology 1985;157(1):157–66.
[143] Sharif HS, Aideyan OA, Clark DC, et al. Brucellar and tuberculous spondylitis: comparative imaging features. Radiology 1989;171(2):419–25.
[144] Sharif HS, Clark DC, Aabed MY, et al. Granulomatous spinal infections: MR imaging. Radiology 1990;177(1):101–7.
[145] Shih TT, Huang KM, Li YW. Solitary vertebral collapse: distinction between benign and malignant causes using MR patterns. J Magn Reson Imaging 1999;9(5):635–42.
[146] Yuh WT, Zachar CK, Barloon TJ, et al. Vertebral compression fractures: distinction between benign and malignant causes with MR imaging. Radiology 1989;172(1):215–8.
[147] Fu TS, Chen LH, Liao JC, et al. Magnetic resonance imaging characteristics of benign and malignant vertebral fractures. Chang Gung Med J 2004;27(11):808–15.
[148] Kubota T, Yamada K, Ito H, et al. High-resolution imaging of the spine using multidetector-row computed tomography: differentiation between benign and malignant vertebral compression fractures. J Comput Assist Tomogr 2005;29(5):712–9.
[149] Cotten A, Dewatre F, Cortet B, et al. Percutaneous vertebroplasty for osteolytic metastases and myeloma: effects of the percentage of lesion filling and the leakage of methyl methacrylate at clinical follow-up. Radiology 1996;200(2):525–30.
[150] Maynard AS, Jensen ME, Schweickert PA, et al. Value of bone scan imaging in predicting pain relief from percutaneous vertebroplasty in osteoporotic vertebral fractures. AJNR Am J Neuroradiol 2000;21(10):1807–12.
[151] Cheung G, Chow E, Holden L, et al. Percutaneous vertebroplasty in patients with intractable pain from osteoporotic or metastatic fractures: a prospective study using quality-of-life assessment. Can Assoc Radiol J 2006;57(1):13–21.
[152] Lieberman IH, Dudeney S, Reinhardt MK, et al. Initial outcome and efficacy of ''kyphoplasty'' in the treatment of painful osteoporotic vertebral compression fractures. Spine 2001;26(14):1631–8.
[153] Masala S, Schillaci O, Massari F, et al. MRI and bone scan imaging in the preoperative evaluation of painful vertebral fractures treated with vertebroplasty and kyphoplasty. In Vivo 2005;19(6):1055–60.
[154] Deyo RA, Mirza SK. Trends and variations in the use of spine surgery. Clin Orthop Relat Res 2006;443:139–46.
[155] Atlas SJ, Keller RB, Wu YA, et al. Long-term outcomes of surgical and nonsurgical management of lumbar spinal stenosis: 8 to 10 year results from the Maine lumbar spine study. Spine 2005;30(8):936–43.
[156] Osterman H, Sund R, Seitsalo S, et al. Risk of multiple reoperations after lumbar discectomy: a population-based study. Spine 2003;28(6):621–7.
[157] Javid MJ, Hadar EJ. Long-term follow-up review of patients who underwent laminectomy for lumbar stenosis: a prospective study. J Neurosurg 1998;89(1):1–7.
[158] Niggemeyer O, Strauss JM, Schulitz KP. Comparison of surgical procedures for degenerative lumbar spinal stenosis: a meta-analysis of the literature from 1975 to 1995. Eur Spine J 1997;6(6):423–9.
[159] Shah RR, Mohammed S, Saifuddin A, et al. Comparison of plain radiographs with CT scan to evaluate interbody fusion following the use of titanium interbody cages and transpedicular instrumentation. Eur Spine J 2003;12(4):378–85.
[160] Bundschuh CV, Modic MT, Ross JS, et al. Epidural fibrosis and recurrent disk herniation in the lumbar spine: MR imaging assessment. AJR Am J Roentgenol 1988;150(4):923–32.
[161] Jorgensen J, Hansen PH, Steenskov V, et al. A clinical and radiological study of chronic lower spinal arachnoiditis. Neuroradiology 1975;9(3):139–44.
[162] Ross JS, Masaryk TJ, Modic MT, et al. MR imaging of lumbar arachnoiditis. AJR Am J Roentgenol 1987;149(5):1025–32.

[163] Zhang H, He M, Mao B. Thoracic spine extradural arteriovenous fistula: case report and review of the literature. Surg Neurol 2006;66(Suppl 1):S18–23.
[164] Kim LJ, Spetzler RF. Classification and surgical management of spinal arteriovenous lesions: arteriovenous fistulae and arteriovenous malformations. Neurosurgery 2006; 59(5 Suppl 3):S195–201.
[165] Spetzler RF, Detwiler PW, Riina HA, et al. Modified classification of spinal cord vascular lesions. J Neurosurg 2002;96(Suppl 2):145–56.
[166] Zozulya YP, Slin'ko EI, Al Qashqish II. Spinal arteriovenous malformations: new classification and surgical treatment. Neurosurg Focus 2006;20(5):E7.
[167] Larsson EM, Desai P, Hardin CW, et al. Venous infarction of the spinal cord resulting from dural arteriovenous fistula: MR imaging findings. AJNR Am J Neuroradiol 1991;12(4): 739–43.
[168] Jones BV, Ernst RJ, Tomsick TA, et al. Spinal dural arteriovenous fistulas: recognizing the spectrum of magnetic resonance imaging findings. J Spinal Cord Med 1997;20(1):43–8.
[169] Bowen BC, Fraser K, Kochan JP, et al. Spinal dural arteriovenous fistulas: evaluation with MR angiography. AJNR Am J Neuroradiol 1995;16(10):2029–43.
[170] Lai PH, Weng MJ, Lee KW, et al. Multidetector CT angiography in diagnosing type I and type IVA spinal vascular malformations. AJNR Am J Neuroradiol 2006;27(4):813–7.
[171] Mascalchi M, Ferrito G, Quilici N, et al. Spinal vascular malformations: MR angiography after treatment. Radiology 2001;219(2):346–53.